



ANTEC<sup>®</sup> 2021

2021 PROCEEDINGS

# FIBER ORIENTATION MEASUREMENTS FOR LARGE ADDITIVE MANUFACTURED PARTS USING OPTICAL AND SEM IMAGING

*Rifat Ara Nargis and David A. Jack  
Baylor University, Waco, Texas*

## Abstract

Acrylonitrile Butadiene Styrene (ABS) is widely used in additive manufactured part production due to its widespread availability and ease of manufacturing, but unfortunately its structural and thermal performance limits its use in industrial applications. The addition of fiber reinforcements, specially chopped carbon fiber to the ABS matrix has the potential to enhance its structural performance while simultaneously reducing dimensional variations during thermal changes. The quantification of the fiber orientation in the processed ABS bead is important to understand its correlation to the mechanical and structural properties of the processed thermoplastic. This study presents the sample preparation and acquisition of images of fiber orientation and void measurements through optical and scanning electron microscopy of an additive manufactured bead with 13% by weight carbon fiber reinforced ABS. The images are then analyzed, and the fiber orientation is measured using the method of ellipses. The method of ellipses poses a problem of ambiguity for the direction of fiber orientation. With the SEM images the ambiguity problem can be solved using an electrical shadowing technique and the orientation of the fibers in the ABS matrix can be determined. The results for the orientation from the two methods are contrasted, and a discussion is provided on the impact the fiber orientation has on the final part performance. The results also indicate the presence of voids caused by the deposition process that is unique to the currently employed additive manufacturing process which will hamper the final part performance.

## 1. Introduction

Acrylonitrile Butadiene Styrene (ABS) is broadly used in additive manufactured part production. ABS consists of butadiene rubber dispersed in a poly styrene-co-acrylonitrile matrix [1]. ABS has an improved toughness relative to many mass produced polymer blends that require processing temperatures below 250°C. But the structural and thermal performance of ABS is limited. The addition of fiber

reinforcements, specifically carbon fibers, allows for enhanced structural performance while simultaneously reducing dimensional variations during thermal changes. A carbon fiber filled thermoplastic also shows significant design tailorability and low cost [2]. The quantification of the fiber orientation in the processed ABS bead is essential to understanding the as manufactured mechanical, thermal, and structural properties of the final part [3].

Optical microscopy is one of the most common methods for determining the fiber orientation in fiber reinforced composite material system. To use optical microscopy, it is essential to obtain high quality images with a high contrast between the fibers and the surrounding matrix [3]. In this present research paper, a 750x digital Dino Lite optical microscope was used to obtain fiber orientation measurement alignment of the polished sample.

One of the most popular methods to measure the fiber orientation in a polymer matrix is the method of ellipses [4]. In this method, the characteristic values of complete and incomplete elliptical footprints are determined, and fiber orientations are measured from these micrographs [5]. But the method of ellipses has its own limitations. The main limitation of MoE is the ambiguity problem which is caused by the fact that every elliptical footprint can represent two different orientation states [6]. Normally, the standard method of ellipses for circular fibers produces a single ambiguity on the resulting fiber orientation. For elliptical cross section fibers there can exist two ambiguities due to the additional degree-of-freedom of roll about the fiber axis [7]. For the material system studied in the present paper, the fibers are circular, and this issue is not considered.

SEM generates images of a sample by scanning the surface with electron beams. The electrons of the beam inside the SEM excites the atoms and stimulates emission of high-energy backscattered electrons and low-energy secondary electrons from the surface of the sample and produces appropriate signals [8]. From the reflected signal, the SEM provides data on surface topology and composition of the sample [9]. SEM is

capable of generating three-dimensional-like images of the surface with the help of large depth of field and shadow relief effect of the secondary and backscattered electron contrast [10]. The JEOL SEM used in this study can go up to 300,000x in magnification. The SEM will be used in this study to produce electrical surface maps that will be analyzed to quantify the direction of each fiber in the etched surface.

## 2. Sample preparation

Sample preparation steps include 3D printing chopped carbon fiber filled ABS on a large FDM system, cutting, making molds for polisher, polishing, cleaning, and etching processes.

### 2.1 3D printing:

Baylor's "Large Area Additive Manufacturing" system, shown in Fig. 1, uses chopped carbon fiber filled ABS beads to print the samples. The 13% by weight carbon fiber filled ABS beads are dried for 4 hours in 80-85 degree centigrade and then kept in a dry environmental chamber at room temperature in air with a dew point of -40°C until testing. The samples are composed of four layers of ABS strips deposited directly on top of each other in the LAAM system. The samples in this study are typically 9 mm wide by 12 mm tall, with each layer being 3 mm in height. In Fig. 2, one of the four-layer ABS strips used in this study is shown. The strips are formed by placing successive layers on top of each other along the same direction for each pass.



Fig. 1. Baylor's LAAM system



Fig. 2. Test specimen with 13% weight fraction carbon fiber ABS

### 2.2 Sample Cutting:

Cutting the sample must be done in such a manner that minimal fiber breakage is introduced and there is not a deforming of the polymer matrix that induces a change of the fiber orientation. This latter scenario can occur if the cutting process produces heat in the sample thereby softening the matrix [3]. The samples for this study are cut with a low speed saw to achieve this goal. The low speed saw maintains the fiber breakage to a minimum and induces a minimal distortion of the fiber shapes on the cut surface. Also, low speed saw cutting keeps the temperature down, so that no form change of the matrix can happen. Fig. 3 shows the sectioned and unpolished sample in an optical image.

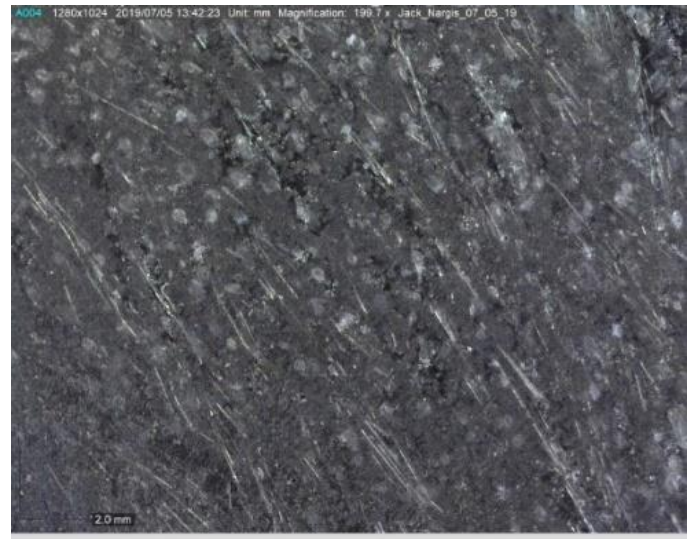


Fig. 3. Sectioned and unpolished specimen

### 2.3 Sample Polishing:

Polishing the sample is a very important step to remove all the damaged fibers in the cutting operation. To prepare the sample for the polisher, the sectioned samples are placed face down in 25 mm diameter molds. Resins and hardener are mixed and poured in the molds and allowed to cure for 6 hours prior to polishing. The final resin mold with a sample inside is shown in Fig. 4. This sample is polished with a Buehler EcoMat 3000 variable speed grinder automatic polisher with 120, 320, 400 and 600 grade silicon carbide electro coated abrasive sandpaper. The sample is polished with 120 grade sandpaper for two minutes, 320 grade for three minutes, 400 grade for 4 minutes and 600 grade for 6 minutes.

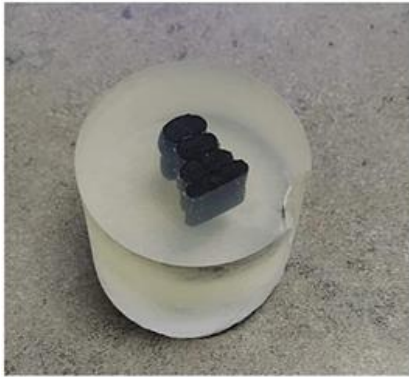


Fig. 4. Sample made for polishing

Next, the sample is polished with micro-cloth and Alumina polishing compound of three different grits, 5-micron, 1 micron and 0.5 micron. Then fine polishing is performed with a final polishing cloth and Alumina polishing compounds of 5-micron, 1 micron and 0.5 micron are used in subsequent steps. In the fine polishing steps, each step was 1 hour long, and polishing compounds are added every 10 minutes. In all polishing steps, a wet environment is maintained to avoid excessive fiber breakage. The wet environment also helps with the removal of debris from the previous steps [3]. This final polishing steps with micro cloth and final polishing cloth provides optimal footprint border [3].

#### 2.4 Sample Cleaning and Etching:

During polishing the sample is cleaned with Harson sonicator ultrasound cleaner, every 10 minutes to remove any debris and clean the surface to make it ready for the microscopes. The ultrasound cleaner used in this study is a Bronson 1510. Ultrasound polishing compound mixed with water is used as the cleaning agent.

The sample is etched with a Plasma-Etch PS-50 for 40-50 minutes in an oxygen with CF<sub>4</sub> gas mixed at a ratio of 3:1.

The plasma reacts with the gases that are present in the chamber and creates volatile etch products. The plasma burns off the ABS and while causing a minimal etch of the carbon fibers. As a result, the fibers stick out from the polymer matrix and creating a better contrast while imaging.

### 3. Image Acquisition from Optical Microscope

A 750x digital Dino Lite optical microscope was used to acquire a qualitative estimate of alignment of the polished sample with the setup shown in Fig. 5. The long working distance and large depth of field provides clear images and the polarizer allows an enhanced contrast of the fibers in the ABS matrix.



Fig. 5. 750X Digital Dino Lite

In Fig. 6, an optical image of the polished sample is shown at a 20x magnification. As the sample has four layers, one layer is divided into nine sections to show the difference in orientation at different areas.



Fig. 6. Image of the surface of the polished sample

For different variation in surface roughness, each image should be taken at their appropriate focus level

with necessary changes in the overall setting. A 750x magnification image of the polished sample is shown in Fig. 7, where we can see the fibers and the voids present in the ABS matrix.



Fig. 7. Image of the polished sample from 750X Dino Lite (Area 5)

From the optical image we can determine how the fibers are positioned in the matrix, but it is difficult to distinguish the correct direction due to ambiguity problem and also the limited resolution. Moreover, from the optical image the presence of voids of varying sizes can be observed.

#### 4. Image Acquisition from Scanning Electron Microscope

A JEOL JSM-6610LV Scan Electron Microscope was used to capture high resolution images of the polished sample which is shown in Fig. 8.



Fig. 8. JEOL JSM-6610LV Scanning Electron Microscope

As shown in Fig. 6, one layer of the sample is divided into nine areas. In Fig. 9, the image acquired from scanning electron microscope of region 4, which is the center-left part of the layer, is shown. We can see that the fibers are neither uniformly distributed spatially and are banded in their orientation behavior. This latter observation is made based upon viewing of the variations in the cross sectioned ellipses. It is also clear that there are significant voids present.

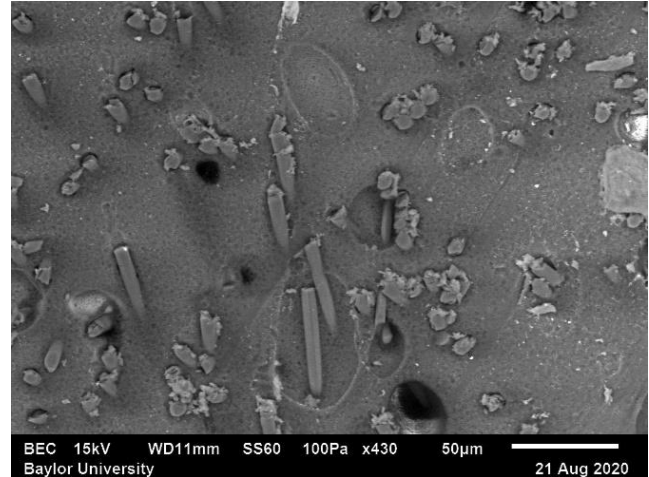


Fig. 9. Image of the center-left part of the surface of the polished sample from SEM (Region 4)

In Fig. 10, the SEM image of region 5 is shown, which is the center-middle part of the layer of the sample. Here, the fibers are mostly oriented towards the out of plane direction of the surface. Thus, we have more circular shapes of the cut fibers. Also, we can notice more voids that are also measurably larger than in region 4. Similar orientation tensors can be found in regions 1, 3, 7 and 9.

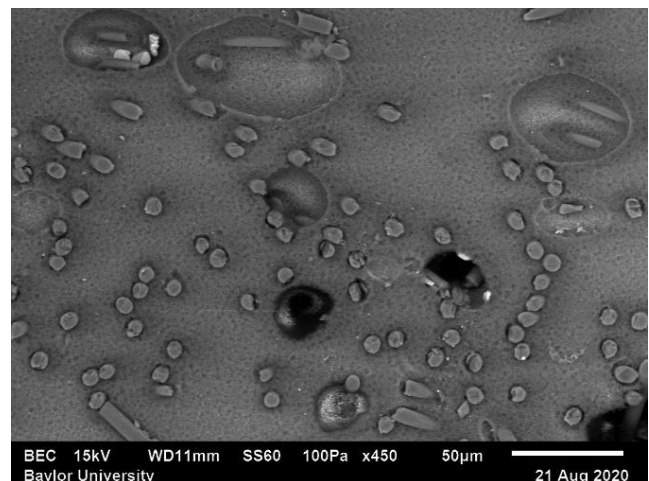


Fig. 10. Image of the center-middle part of the surface of the polished sample from SEM (Region 5)

Fig. 11 shows the SEM image of region 6, which is the center-right area of the layer. There are fewer voids present in this relative to the other regions. But the fibers are more randomly oriented and long ellipses from the cut fibers are observed.

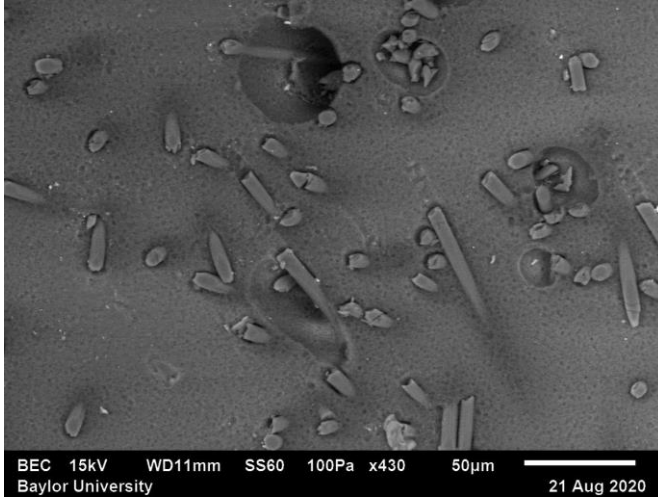


Fig. 11. Image of the center-right part of the surface of the polished sample from SEM (Region 6)

## 5. Method Used for The Quantification of Fiber Orientation

The method of ellipses (MoE) is used to determine the orientation of the fibers. In MoE, the orientation of the fibers is obtained from the characteristic values of complete or incomplete elliptical footprints and rectangular footprints seen in micrographs [3].

$$\theta_f = \cos^{-1}(m/M) \quad (1)$$

Where,  $m$  is the minor axis,  $M$  is the major axis and  $\theta_f$  is the out of plane angle [2]. In Fig. 12, the definition of geometrical parameters in MoE is shown, the coordinate of which follow that of Velez-Garcia [2].

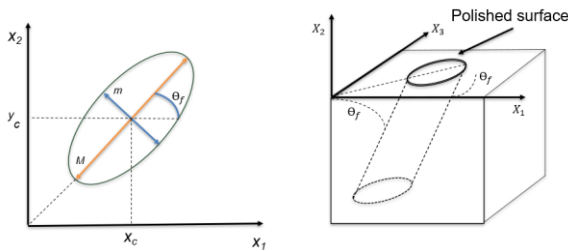


Fig. 12. Definition of geometrical parameters in MoE (image inspired from [3])

The equations of the projected ellipse of an cylinder onto a viewing plane are determined in terms of the semi-major and semi-minor diameters [7]. Fiber angles are determined by numerical fitting of the developed equations to measured ellipses.

The components of the tensor  $A_{ij}$  per unit volume of material in the area inspected are obtained using a weighted average [6]:

$$A_{ij} = \frac{\sum_n (p_i p_j)_n L_n F_n}{\sum_n L_n F_n} \quad (2)$$

Here,  $p_i$  = the  $i^{\text{th}}$  direction of the orientation unit vector corresponding to the axis of the fiber

$L_n$  = length of the fiber (experimentally found to be 341  $\mu\text{m}$  in the companion study)

$d$  = diameter of the fiber (experimentally found to be 6.37  $\mu\text{m}$  in the companion study)

$F_n$  = the weighting function that relates the orientation per unit area to the orientation per unit volume, where

$$F_n = \frac{1}{L_n \cos(\theta_f)_n + d_n \sin(\theta_f)_n} \quad (3)$$

where  $d_n$  is the diameter of the  $n^{\text{th}}$  fiber,  $i = 1-3, j = 1-3$ ; (for  $X_1, X_2$  and  $X_3$  plane)

The value of  $A_{ij}$  can be from 0 to 1. 1 indicating the highest alignment towards a plane.

## 6. Results

Every fiber is traced, and an outline is created for the cross-sectional area of the fiber. A simple optimization algorithm is then used to identify the best-fit, in the least squares sense, ellipsoid to the fiber cross section. The major and minor axis lengths along with the direction of the major axis is extracted from the best fit ellipse and this information is then used to evaluate Equation (2) for the orientation tensor  $A_{ij}$ . Fig. 13 shows the tracing of each fiber on the surface of Region 7 from the layer in the sample.

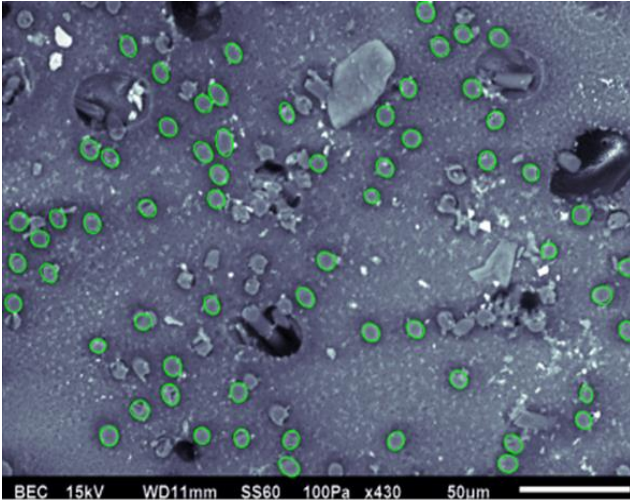


Fig. 13. Fiber orientation measurement by MoE (Region 7)

In Table 1, the orientation tensor value from each of the regions shown in Fig. 6 is presented.

Area	Fiber Count	$A_{11}$	$A_{22}$	$A_{33}$
1	65	0.13	0.17	0.71
2	28	0.21	0.43	0.36
3	55	0.31	0.07	0.62
4	40	0.27	0.18	0.55
5	53	0.14	0.21	0.65
6	38	0.31	0.18	0.51
7	54	0.12	0.16	0.72
8	35	0.37	0.13	0.50
9	45	0.30	0.09	0.61

Table 1. Orientation tensor for different areas of the sample.

From the fiber orientation measurement, it is evident that fibers are most aligned towards the  $X_3$  direction, the direction of deposition, at regions 1,3,5,7 and 9. At the corners of the deposited bead the orientation state tends toward random, clearly indicating significant spatial inhomogeneity of the orientation state within the individual deposited bead.

The SEM generates much clearer and a three-dimensional-like image due to secondary and

backscattered contrast of a surface. In the SEM image, under-surface shadow of each fiber can be traced, thus the actual orientation of each fiber in the matrix can be determined. It resolves the ambiguity problem that was the main concern with optical microscopy. This can be observed in Fig. 14 of Region 2. Notice that each of the fibers has a contrasting shadow for the part of the fiber that lies under the surface.

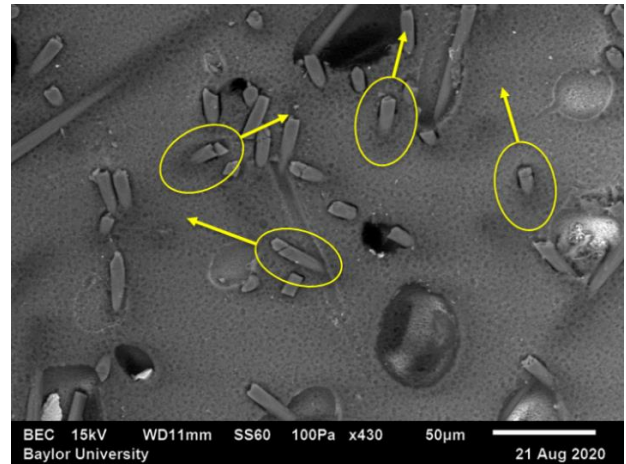


Fig. 14. Tracing under surface shadow of fiber to determine orientation (Region 2)

In both optical and SEM images, the presence of voids in the ABS matrix is found. The presence of voids significantly impacts the mechanical and thermal properties negatively of the chopped carbon fiber filled ABS. In Fig. 15, a zoomed in view of Region 8, shows the clear presence of voids within the matrix. These voids would not be present in injection or compression molded composites due to the presence of high packing pressures, but due to the die swell and lower pressures used within the FDM process voids can easily form during processing.

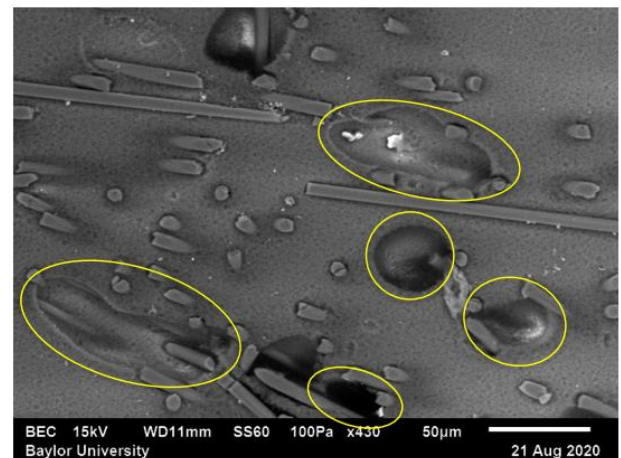


Fig. 15. Void determination

Impact of fiber orientation on mechanical and thermal properties are:

1. The stiffness is the highest at the middle and near surface regions where the fibers are the most aligned compared to the low aligned area.
2. The coefficient of thermal expansion will be the lowest at the middle where the fibers are the most aligned compared to the low aligned area.

This result supports the findings of the previous works [11] qualitatively, but there is further work needed for a quantitative comparison due to the difference between the measured and predicted values for orientation. In this study there is also the presence of voids that can be accurately characterized and is the scope of future research.

## 7. Conclusions

The fibers experience their greatest alignment in the center and near surface regions of the deposited bead in the direction of the printed bead. The orientation of the fibers directly impact the mechanical, structural and thermal properties of the thermoplastic, and a quantitative comparison between the actual part's orientation and the predicted orientation state will provide guidance when looking to improve the as processed part quality in comparison to the as-designed performance.

## 8. Acknowledgements

The authors wish to express their gratitude to Dr. Gregorio Velez-Garcia who provided advice on the proper technique for sectioning and polishing the samples.

## References

[1] Olaf Meincke, Drik Kaempfer, Hans Weikmann, Christian Friedrich, Marc Vathauer, Holger Warth; February 2004; "Mechanical properties and electrical conductivity of carbon-nanotube filled polyamide-6 and its blends with acrylonitrile/butadiene/styrene".

[2] L.G. Blok, M.L. Longana, H. Yu and B.K.S. Woods; August 2018; "An investigation into 3D printing of fiber reinforced thermoplastic composites"

[3] G.M. Velez-Garcia, P. Wapperom, V. Kunc, D.G. Baird & A. Zink-Sharp; June 2012; "Sample Preparation and Image Acquisition Using Optical-Reflective Microscopy in the Measurement of Fiber Orientation in Thermoplastic Composites".

[4] G. Fischer, P. Eyerer; 1988; "Measuring spatial orientation of short fiber reinforced thermoplastics by image analysis."

[5] Gregorio Manuel Vélez-García; January 2012; "Experimental Evaluation and Simulations of Fiber Orientation in Injection Molding of Polymers Containing Short Glass Fibers".

[6] G.M. Vélez-García, P. Wapperom, D. Baird, A.O. Aning, V. Kunc; 2012; "Unambiguous orientation in short fiber composites over small sampling area in a center gated disk."

[7] Nathan D. Sharp, Johnathan E. Goodsell and Anthony J. Favaloro; March 2019; "Measuring Fiber Orientation of Elliptical Fibers from Optical Microscopy."

[8] Joseph Goldstein, Dale E. Newbury, David C. Joy, Charles E. Lyman, Patrick Echlin, Eric Lifshin, Linda Sawyer, J.R. Michael; 2003; "Scanning Electron Microscopy and X-Ray Microanalysis: Third Edition 3rd Edition".

[10] Goldstein, J., Newbury, D.E., Joy, D.C., Lyman, C.E., Echlin, P., Lifshin, E., Sawyer, L., Michael, J.R.; 2003; "Scanning Electron Microscopy and X-Ray Microanalysis: Third Edition".

[11] Timothy Russell, Blake Heller, David A. Jack and Douglas E. Smith; March 2018; "Prediction of the Fiber Orientation State and the Resulting Structural and Thermal Properties of Fiber Reinforced Additive Manufactured Composites Fabricated Using the Big Area Additive Manufacturing Process".